Electronic Supplementary Material (ESI) for Environmental Science: Nano.
This journal is © The Royal Society of Chemistry 2022

Supplemental Information

Dual Metal Co-anchored Nanosheet to Catalyze Advanced Oxidation Processes for Highly Efficient Oxytetracycline Degradation

Meng Li [a, b], Jian-Fang Yan [b], Zhao-Xin Zhang [d], Wei Han [c], Shao-Qi Zhou [e, *], King Lun Yeung [a, c, *], Ce-Hui Mo [b, *]

a. Department of Chemical and Biological Engineering, The Hong Kong University of Science and Technology, Clear Water Bay, Kowloon, Hong Kong SAR, PR. China

b. Guangdong Provincial Research Center for Environment Pollution Control and Remediation Materials, College of Life Science and Technology, Jinan University, Guangzhou 510632, PR. China.

c. Division of Environment and Sustainability, The Hong Kong University of Science and Technology, Clear Water Bay, Kowloon, Hong Kong SAR, PR. China

d. Thrust of Sustainable Energy & Environment, The Hong Kong University of Science and Technology (Guangzhou), Guangzhou, 511458, PR China

e. College of Resources and Environmental Engineering, Guizhou University, 2708 Huaxi Road, Guiyang 550025, PR. China

* Corresponding Author.

E-mail address: kemengli@ust.hk (M. Li); fesqzhou@126.com (S. Zhou); kekyeung@ust.hk (K.L. Yeung); tchmo@jnu.edu.cn (C. Mo).

Supplemental Text

Text S1. Chemicals

Melamine ($C_3H_6N_6$), ferric chloride hexahydrate ($FeCl_3 \cdot 6H_2O$), cobalt chloride hexahydrate ($CoCl_2 \cdot 6H_2O$), 2-amino terephthalic acid ($C_8H_7NO_4$), N, N-Dimethylformamide (C_3H_7NO, DMF), potassium peroxymonosulfate ($KHSO_5 \cdot 0.5KHSO_4 \cdot 0.5K_2SO_4$, 42.8−46%, PMS), oxytetracycline ($C_{22}H_{24}N_2O_9$, OTC), and 5,5-dimethyl-1-pyrroline N-oxide ($C_6H_{11}NO$, DMPO) were bought from Shanghai Aladdin Biochemical Technology Co., Ltd. Shanghai Macklin Biochemical Co., Ltd. provided the Ethanol (EtOH), tert-butyl alcohol (TBA), sodium sulfate (Na_2SO_4), 1,4-benzoquinone (BQ), L-histidine ($C_6H_9N_3O_2$, LH), sodium chloride (NaCl), bicarbonate ($NaHCO_3$), magnesium sulfate ($MgSO_4$), peptone, ammonia (NH_4Cl), monopotassium phosphate (KH_2PO4) and humic acid (HA). All the chemicals employed in this study were of analytical grade without further purification.

Text S2. Electrochemical measurements

Catalysts inks were prepared by ultrasonically dispersed 2.0 mg of catalyst into a 0.5 mL solution contained 300 uL of methanol, 150 uL of H_2O, and 50 uL of Nafion (5wt%). Subsequently, 7 uL of catalyst ink was drop-cast onto the surface of glassy carbon electrode, and the final modified electrode was air-dried under room temperature. Cyclic voltammetry (CV) was recorded from -0.6 V to 1.0 V at a sweeping rate of 5 mV s^{-1} via an electrochemical workstation with three-electrode system. Electrochemical impedance spectroscopy (EIS) was operated at the frequency range of 100 kHz to 5 mHz at an amplitude 5 mV. Linear sweep voltammetry (LSV) was conducted from 0.2 to 1.6 V at a sweeping rate of 5 mV s^{-1}.

Supplemental Figures

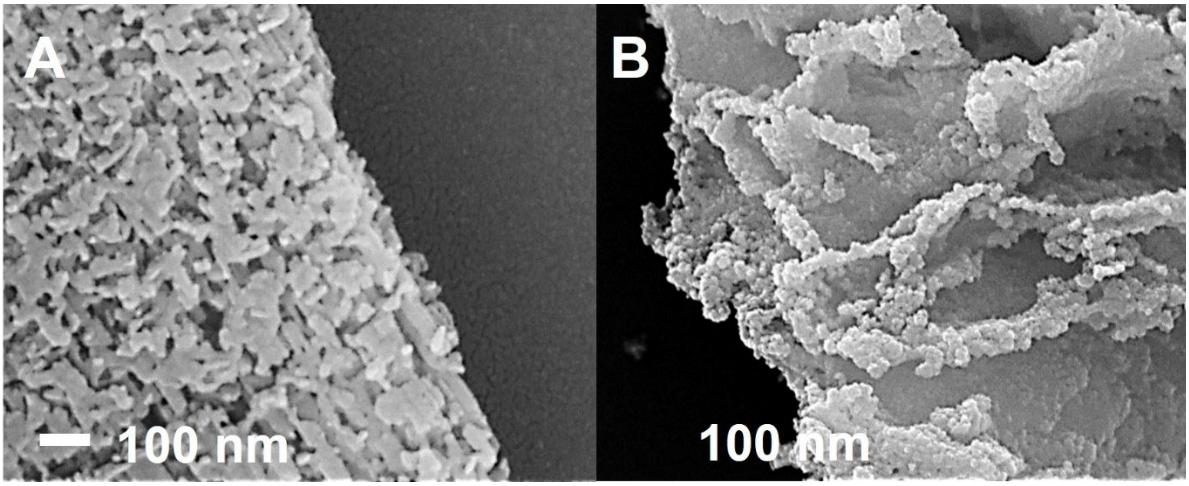

Figure S1. SEM morphologies of (A) g-C_3N_4 and (B) CoFeX.

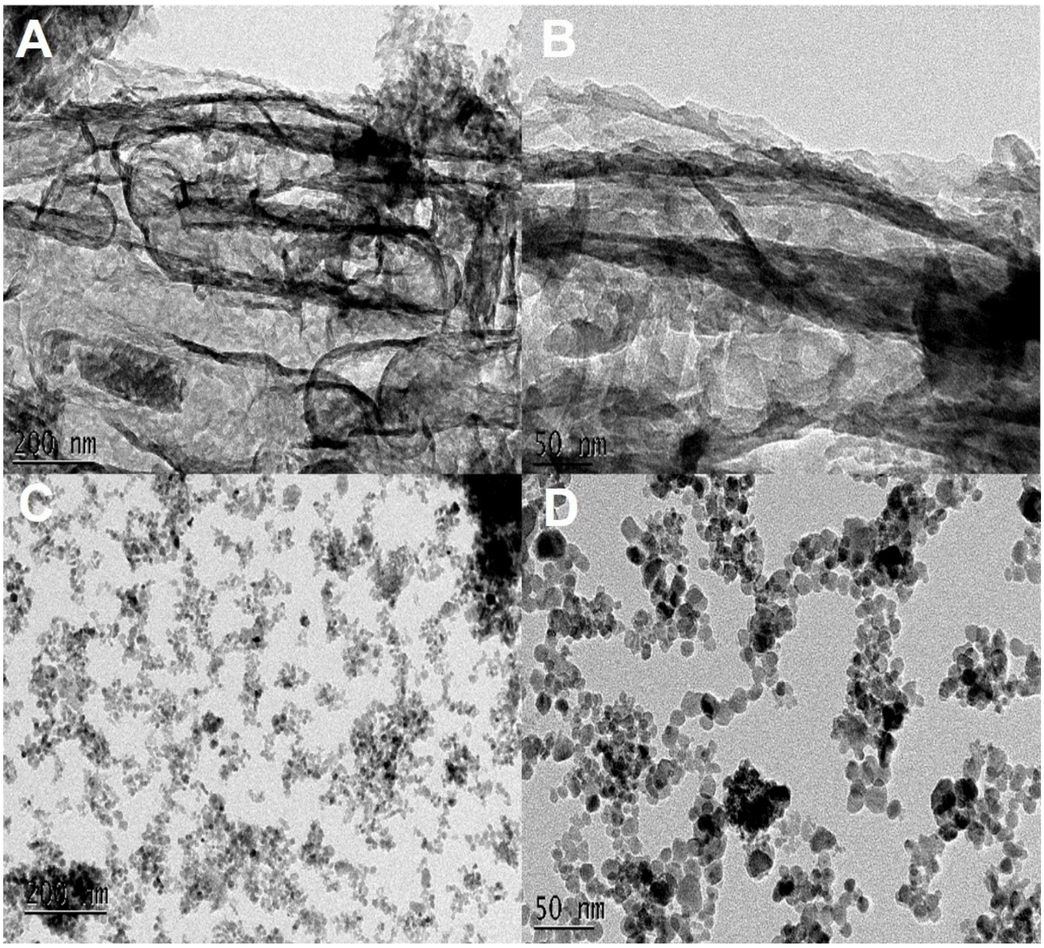

Figure S2. TEM morphologies of (A-B) g-C_3N_4, (C) CoFeX, and (D) 40%-N/CoFeX nanoparticle.

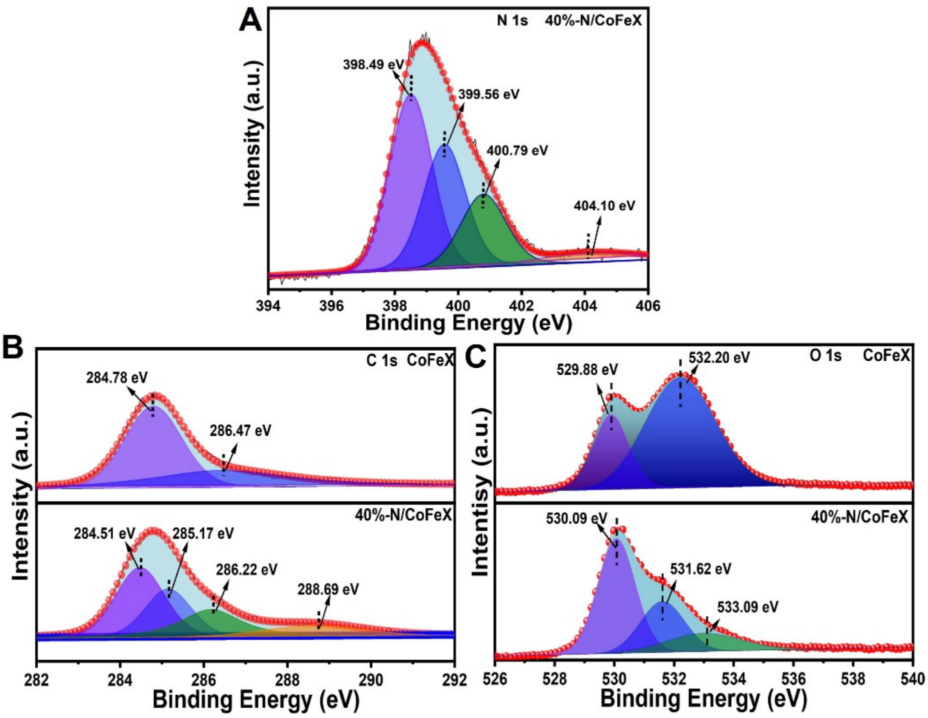

Figure S3. XPS spectra of (A) N 1s, (B) C 1s, and (C) O 1s of CoFeX and 40%-N/CoFeX.

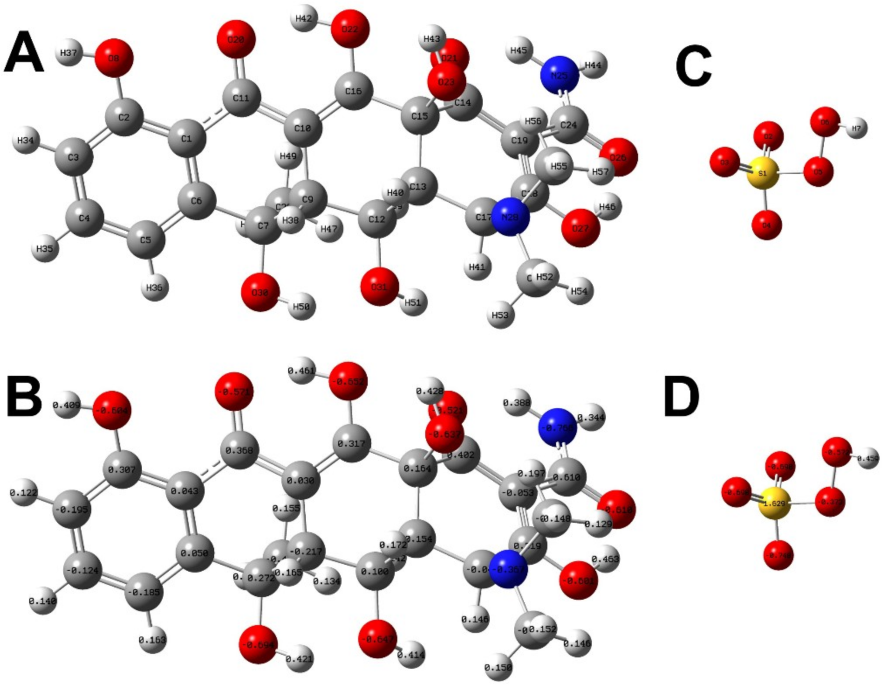

Figure S4 (A) The optimized molecular structure of OTC and (B) the corresponding atomic charge distribution. (C) The optimized molecular structure of PMS and (D) the corresponding atomic charge distribution.

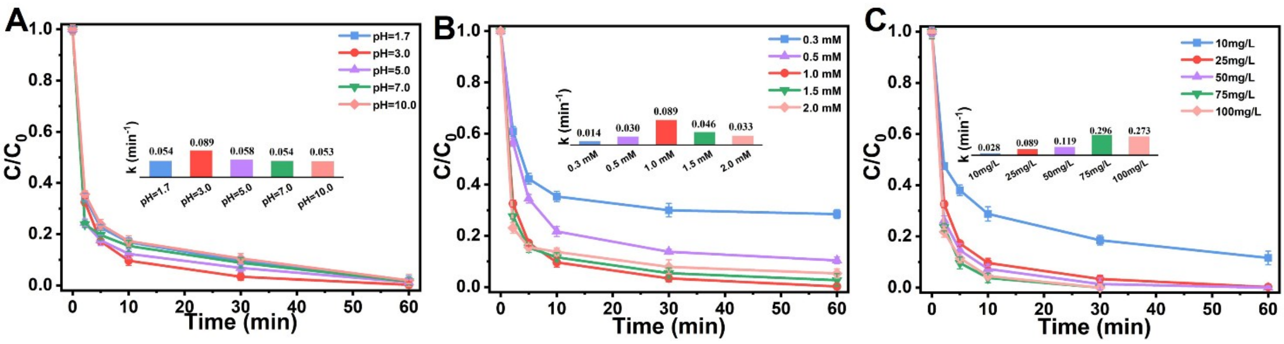

Figure S5. Effects of (A) initial pH values, (B) PMS concentration, and (C) catalysts loading on OTC degradation by 40%-N/CoFeX. General conditions: C_0(OTC) = 100 mg L^{-1}; C_0 (PMS) = 1.0 mM; C_0 (Catalyst) = 25 mg L^{-1}; pH = 3; T = 26ºC.

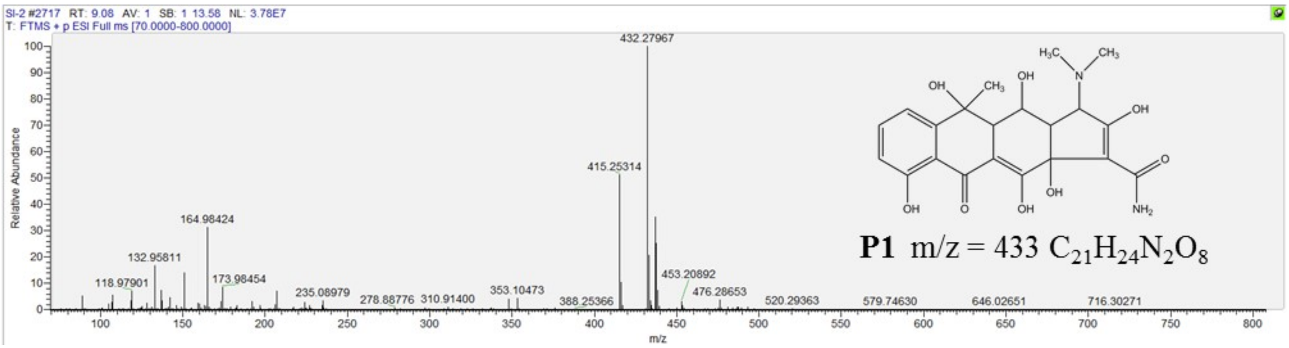
SI-2 #2717 RT: 9.08 AV: 1 SB: 1 13.58 NL: 3.78E7
T: FTMS + p ESI Full ms [70.0000-800.0000]
Relative Abundance
m/z
P1 m/z = 433 $C_{21}H_{24}N_2O_8$

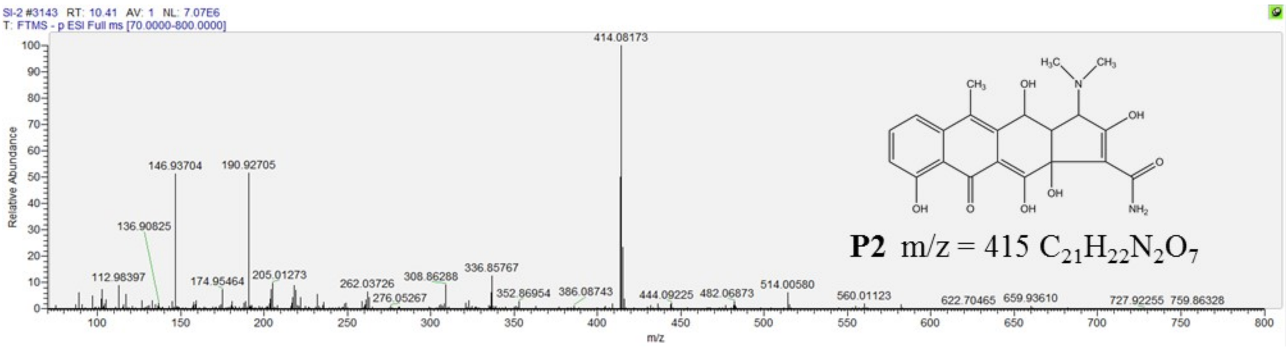
SI-2 #3143 RT: 10.41 AV: 1 NL: 7.07E6
T: FTMS - p ESI Full ms [70.0000-800.0000]
Relative Abundance
m/z
P2 m/z = 415 $C_{21}H_{22}N_2O_7$

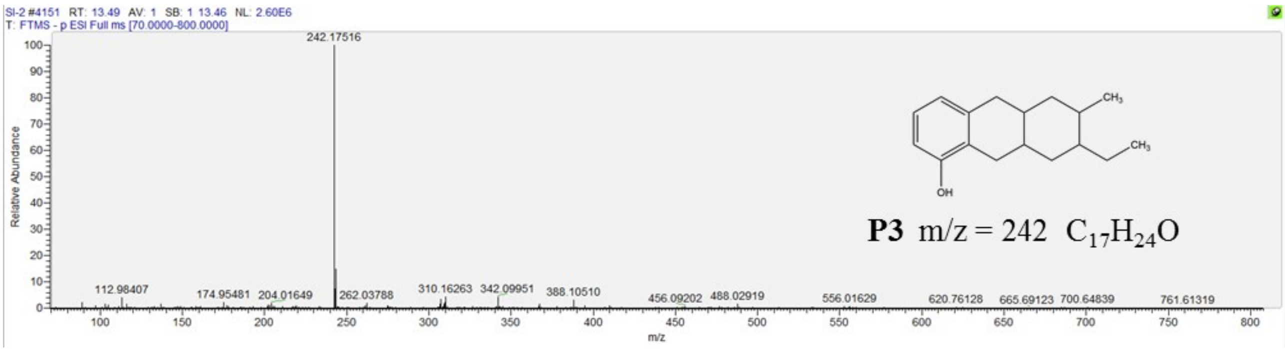
SI-2 #4151 RT: 13.49 AV: 1 SB: 1 13.46 NL: 2.60E6
T: FTMS - p ESI Full ms [70.0000-800.0000]
Relative Abundance
m/z
P3 m/z = 242 $C_{17}H_{24}O$

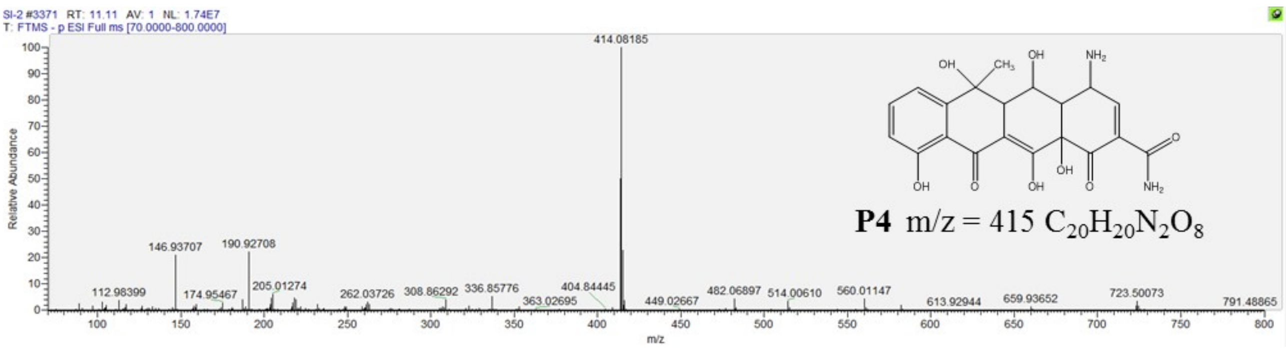
SI-2 #3371 RT: 11.11 AV: 1 NL: 1.74E7
T: FTMS - p ESI Full ms [70.0000-800.0000]
Relative Abundance
m/z
P4 m/z = 415 $C_{20}H_{20}N_2O_8$

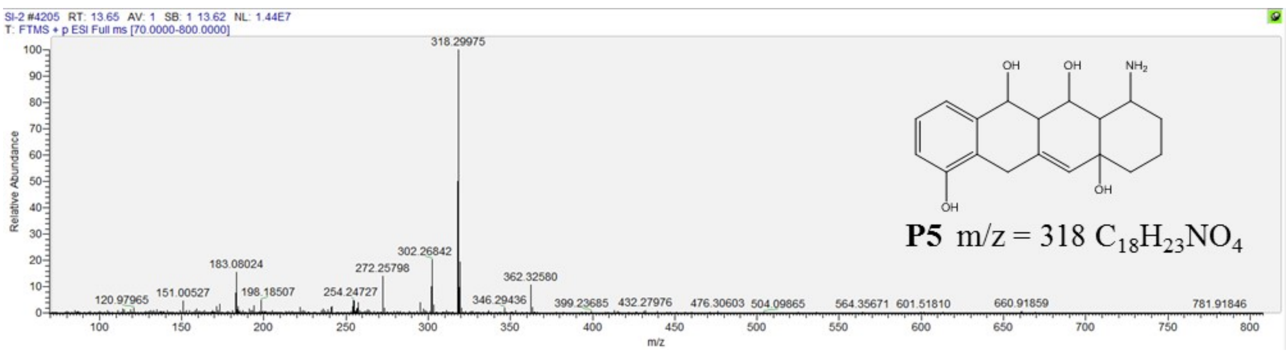
SI-2 #4205 RT: 13.65 AV: 1 SB: 1 13.62 NL: 1.44E7
T: FTMS + p ESI Full ms [70.0000-800.0000]
Relative Abundance
m/z
P5 m/z = 318 $C_{18}H_{23}NO_4$

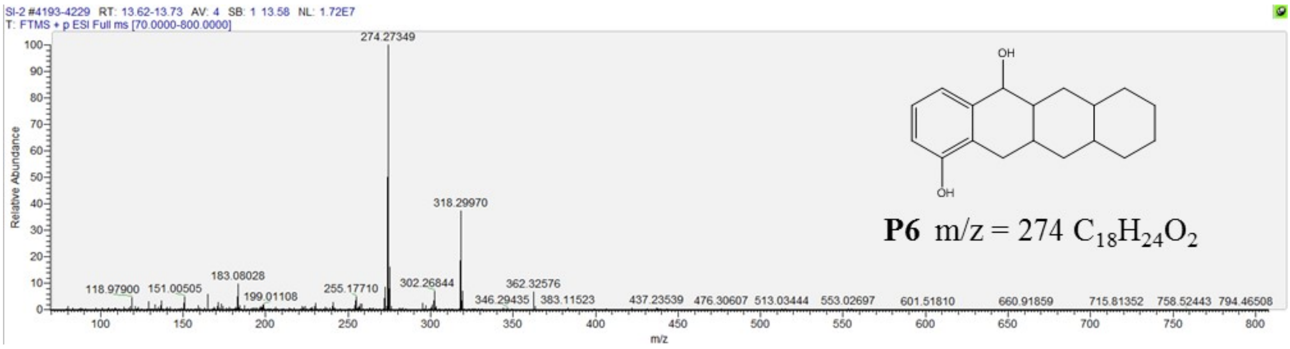
SI-2 #4193-4229 RT: 13.62-13.73 AV: 4 SB: 1 13.58 NL: 1.72E7
T: FTMS + p ESI Full ms [70.0000-800.0000]
Relative Abundance
m/z
274.27349
318.29970
183.08028
302.26844
362.32576
OH
OH
P6 m/z = 274 C18H24O2

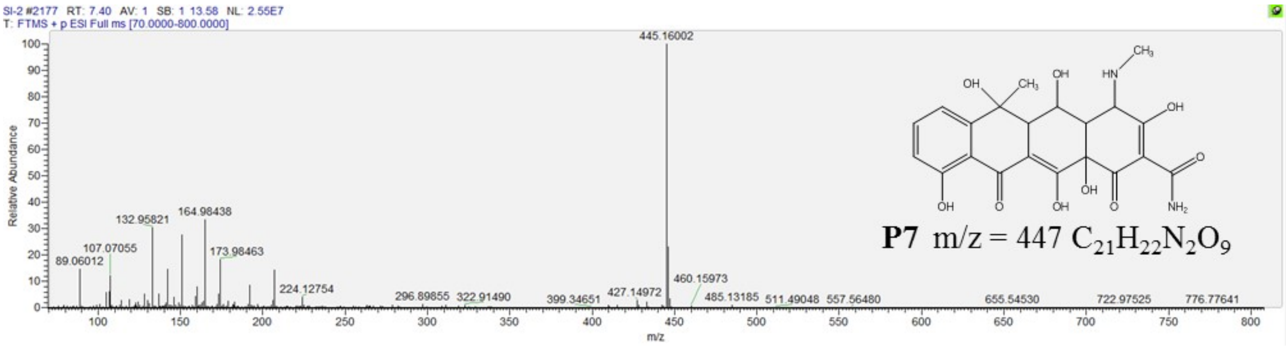
SI-2 #2177 RT: 7.40 AV: 1 SB: 1 13.58 NL: 2.55E7
T: FTMS + p ESI Full ms [70.0000-800.0000]
Relative Abundance
m/z
445.16002
132.95821
164.98438
107.07055
173.98463
89.06012
224.12754
460.15973
P7 m/z = 447 C21H22N2O9

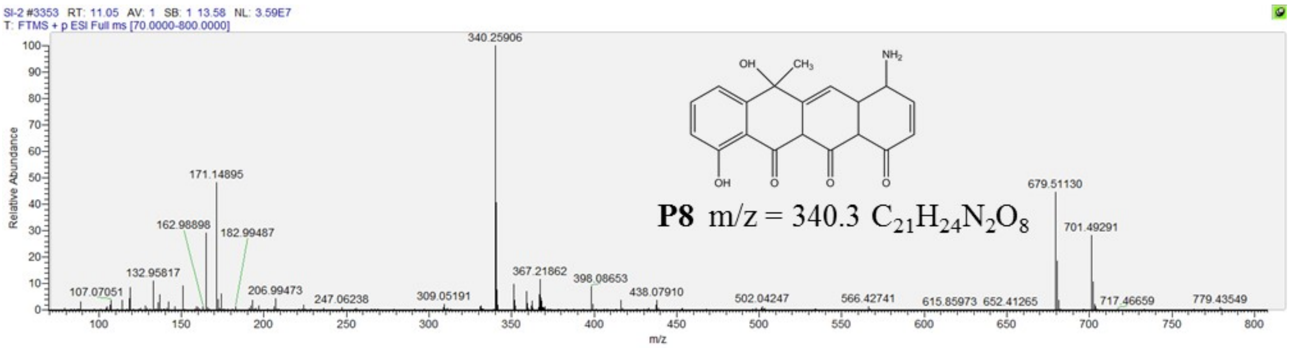
SI-2 #3353 RT: 11.05 AV: 1 SB: 1 13.58 NL: 3.59E7
T: FTMS + p ESI Full ms [70.0000-800.0000]
Relative Abundance
m/z
340.25906
171.14895
162.98898
182.99487
679.51130
701.49291
367.21862
398.08653
P8 m/z = 340.3 C21H24N2O8

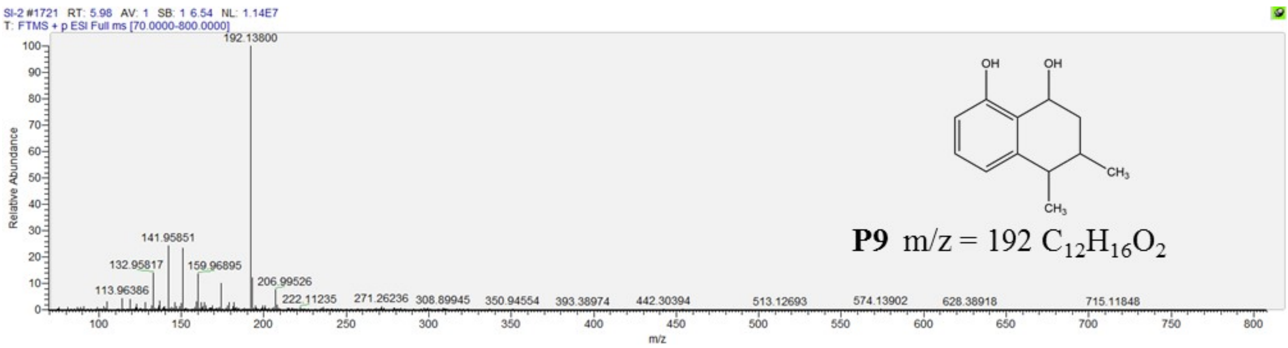
SI-2 #1721 RT: 5.98 AV: 1 SB: 1 6.54 NL: 1.14E7
T: FTMS + p ESI Full ms [70.0000-800.0000]
Relative Abundance
m/z
192.13800
141.95851
132.95817
159.96895
206.99526
P9 m/z = 192 C12H16O2

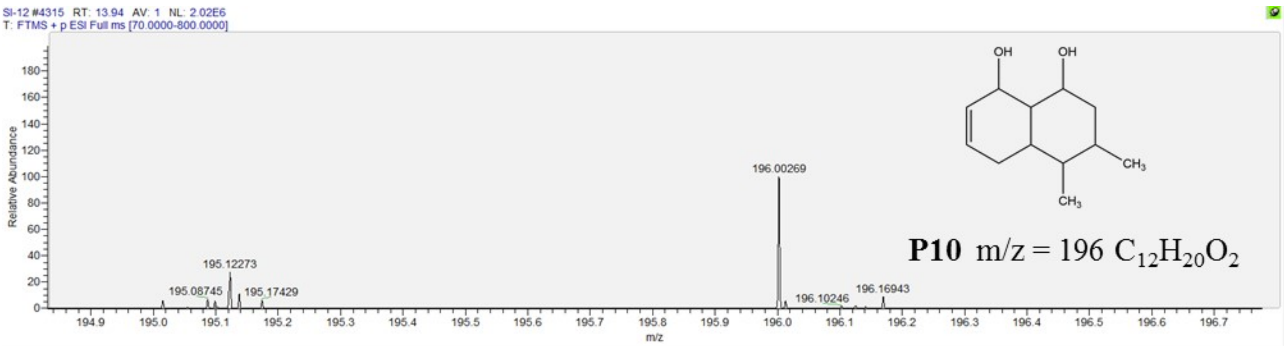
SI-12 #4315 RT: 13.94 AV: 1 NL: 2.02E6
T: FTMS + p ESI Full ms [70.0000-800.0000]
Relative Abundance
m/z
196.00269
195.12273
195.08745
195.17429
196.10246
196.16943
P10 m/z = 196 C12H20O2

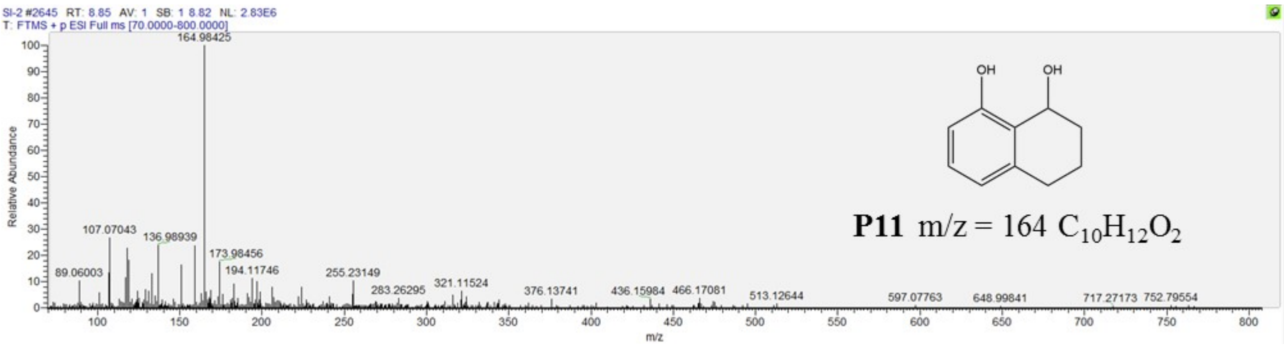

Figure S6. Mass spectra of the degradation intermediates (P1-P11).

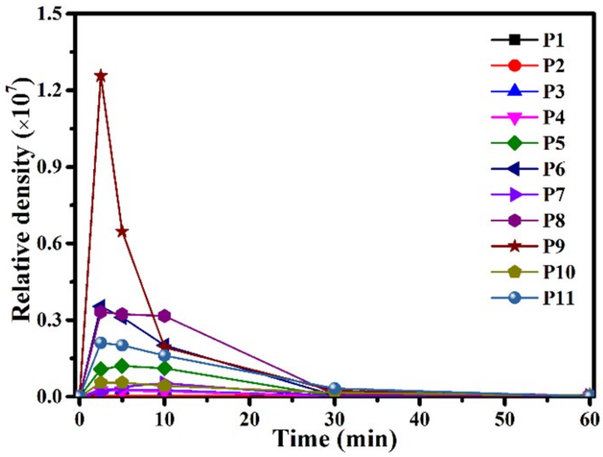

Figure S7 Evolution pattern of degradation intermediates from OTC. General conditions: C_0(OTC) = 100 mg L^{-1}; C_0 (PMS) = 1.0 mM; C_0 (Catalyst) = 25 mg L^{-1}; pH = 3; T = 26ºC.

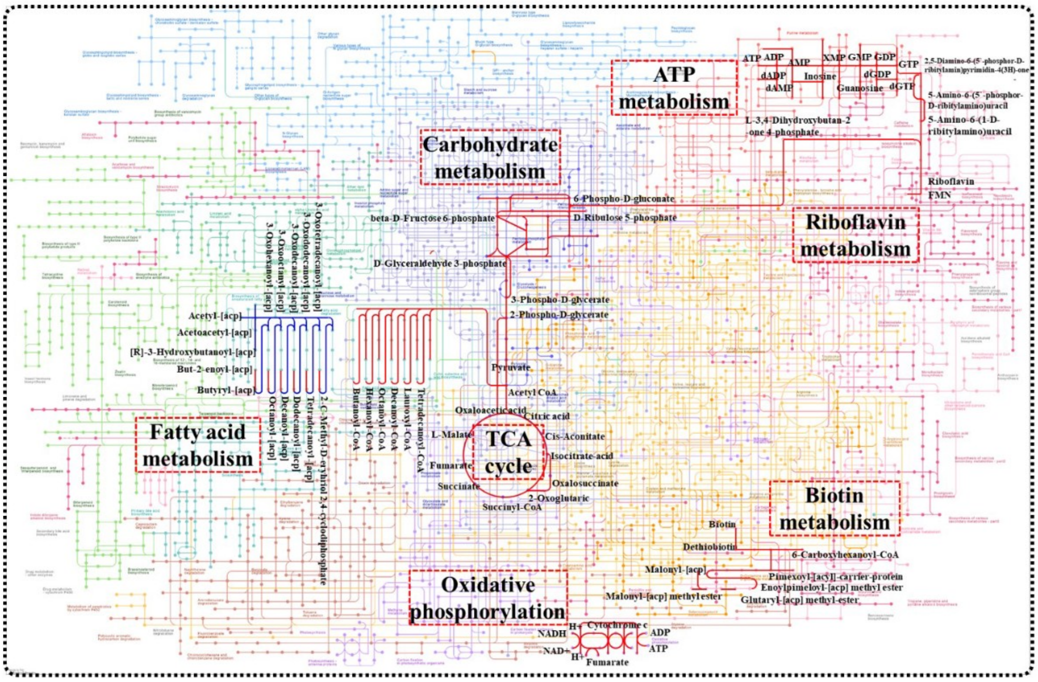

Figure S8. The KEGG metabolism networks associated with differently regulated expression proteins in E coli. exposure to 30 min OTC degradation intermediates compared to OTC (Red and blue lines present the up- and down-regulated metabolism pathway, respectively).

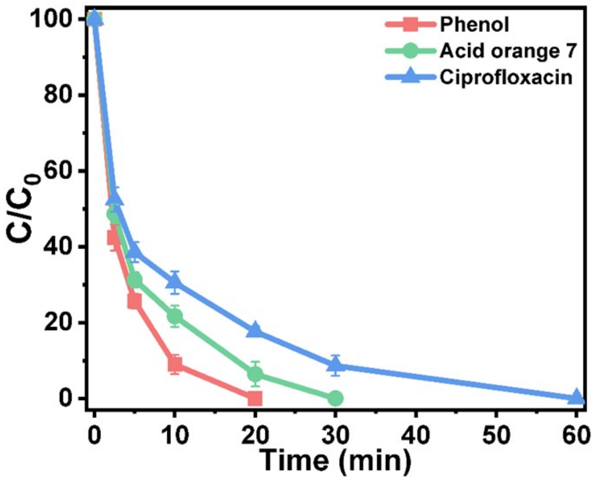

Figure S9. Degradation properties of various organic pollutants (Phenol, Acid orange 7, and Ciprofloxacin) by 40%-N/CoFeX activated PMS. General conditions: C_0 = 100 mg L^{-1}; C_0 (PMS) = 1.0 mM; C_0 (Catalyst) = 25 mg L^{-1}; pH = 3; T = 26ºC.

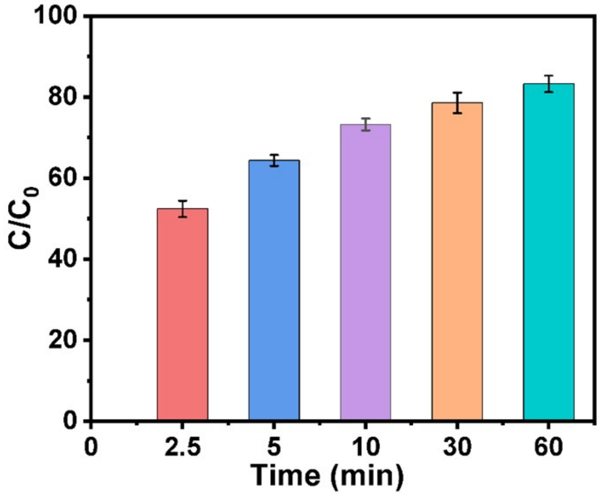

Figure S10. The mineralization efficiency of OTC. General conditions: C_0(OTC) = 100 mg L^{-1}; C_0 (PMS) = 1.0 mM; C_0 (Catalyst) = 25 mg L^{-1}; pH = 3; T = 26ºC.

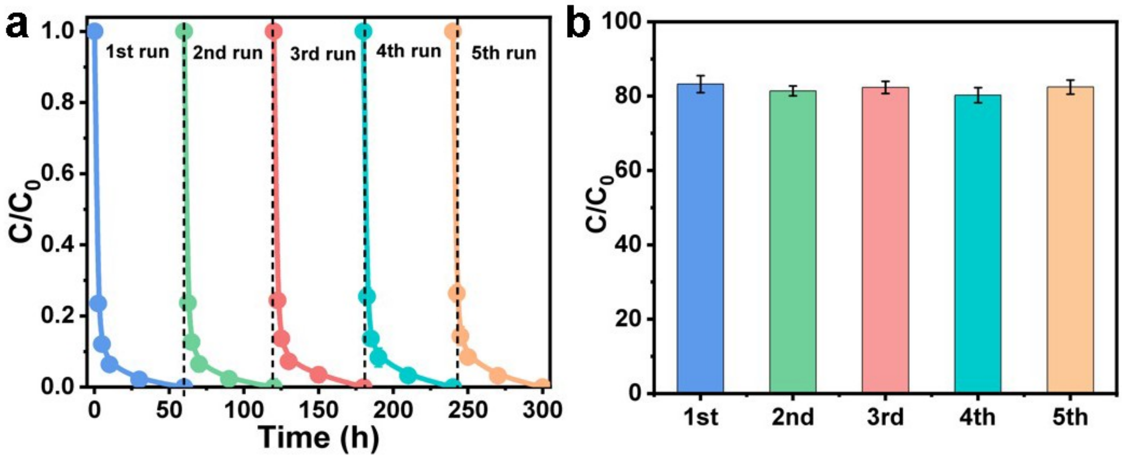

Figure S11. (a) The degradation cycle of OTC when 40%-N/CoFeX was treated and (b) the mineralized efficiency of OTC. General conditions: C_0(OTC) = 100 mg L^{-1}; C_0 (PMS) = 1.0 mM; C_0 (Catalyst) = 25 mg L^{-1}; pH = 3; T = 26ºC.

Supplemental Tables

Table S1 Charge distribution and f⁻ of the optimized structures.

Atom	Site	Charge (0)	Charge (-1)	Charge (+1)	f⁻	f+
C	1	-0.034	-0.013	-0.044	0.021	0.010
C	2	0.092	0.125	0.067	0.033	0.025
C	3	-0.072	-0.038	-0.099	0.034	0.027
C	4	-0.027	0.004	-0.076	0.031	0.049
C	5	-0.054	-0.005	-0.075	0.049	0.021
C	6	0.012	0.025	-0.010	0.013	0.022
C	7	0.087	0.088	0.085	0.001	0.002
O	8	-0.171	-0.120	-0.189	0.051	0.018
C	9	-0.028	-0.025	-0.030	0.003	0.002
C	10	-0.063	-0.041	-0.078	0.022	0.015
C	11	0.133	0.139	0.069	0.006	0.064
C	12	0.058	0.062	0.056	0.004	0.002
C	13	-0.031	-0.025	-0.033	0.006	0.002
C	14	0.129	0.133	0.068	0.004	0.061
C	15	0.072	0.073	0.063	0.001	0.009
C	16	0.101	0.115	0.062	0.014	0.039
C	17	0.021	0.032	-0.044	0.011	0.065
C	18	-0.082	-0.064	-0.098	0.018	0.016
C	19	-0.082	-0.064	-0.098	0.018	0.016
O	20	-0.229	-0.209	-0.297	0.020	0.068
O	21	-0.241	-0.218	-0.291	0.023	0.050
O	22	-0.168	-0.140	-0.204	0.028	0.036
O	23	-0.199	-0.195	-0.223	0.004	0.024
C	24	0.165	0.172	0.155	0.007	0.010
N	25	-0.136	-0.120	-0.152	0.016	0.016
O	26	-0.277	-0.256	-0.305	0.021	0.028
O	27	-0.163	-0.154	-0.207	0.009	0.044
N	28	-0.092	0.030	-0.099	0.122	0.007
C	29	-0.098	-0.093	-0.102	0.005	0.004
O	30	-0.241	-0.229	-0.255	0.012	0.014
O	31	-0.181	-0.172	-0.192	0.009	0.011
C	32	-0.041	-0.015	-0.048	0.026	0.007
C	33	-0.053	-0.028	-0.058	0.025	0.005

Table S2 The surface properties of as-synthesized composites.

Samples	Surface Area ($m^2\ g^{-1}$)	Pore volume ($cm^3\ g^{-1}$)	Average pore diameter (nm)
g-C_3N_4	85.22	0.362	16.99
CoFeX	129.07	0.182	10.54
10%-N/CoFeX	141.81	0.260	7.26
20%-N/CoFeX	144.18	0.400	11.11
40%-N/CoFeX	151.45	0.453	7.34
60%-N/CoFeX	132.44	0.424	11.23
80%-N/CoFeX	96.21	0.340	14.15

Table S3 Comparison of 40%-N/CoFeX with some previously reported catalyst for degradation contaminants in different system.

Catalyst	Reaction condition	Performance (k)	Main ROS	Reference
$CoFe_2O_4$/SAC	Antibiotic norfloxacin /10 mg L^{-1}; Catalyst/100 mg L^{-1}; 150 mg L^{-1}; pH/ 6.0	97.5% in 60 min / 0.035 min^{-1}	·OH; $SO_4^{\cdot-}$	[1]
CoFe double hydroxides	Ciprofloxacin/ 20 mg L^{-1}; Catalyst /50 mg L^{-1}; PMS/0.25 mM; pH/6.8	84.6% in 12 min / 0.043 min^{-1}	·OH; $SO_4^{\cdot-}$	[2]
RGO@$CoFe_2O_4$	Ofloxacin/40 μM; Catalyst/100 mg L^{-1}; PMS/0.1 mM; pH/6.0	100% in 30 min / 0.018 min^{-1}	·OH; $SO_4^{\cdot-}$	[3]
$CuFeO_2$/biochar	Tetracycline/20 mg L^{-1}; Catalyst /200 mg L^{-1}; UV /400 nm; H_2O_2 /20 mM; pH/5.0	100% in 120 min / 0.022 min^{-1}	·OH; ·O- 2	[4]
CuO	Acid orange 7/30 μm; Catalyst/ 1.0 g L^{-1}; PMS/1.0 mM; pH/7.5	100% in 20 min / 0.063 min^{-1}	$^1O_2$	[5]
CoFeLa-LDH	Triclosan/20 μM; Catalyst/20 mg L^{-1}; PMS/ 40 μM; pH/7.0	100 % in 60 min /0.039 min^{-1}	$^1O_2$; ·O- 2	[6]
ZIF-8 B, N, C	Tetracycline/20 mg L^{-1}; Catalyst /5 mg L^{-1}; PMS/15 mg L^{-1}; pH/4.5	97.5 % in 60 min /0.072 min^{-1}	·OH;$SO_4^{\cdot-}$; $^1O_2$; ·O- 2	[7]
	Tetracycline/20 mg L^{-1}; Catalyst/ 5 mg L^{-1}; PMS/15 mg L^{-1}; pH/4.5	98.7 % in 60 min /0.087 min^{-1}	OH;$^1O_2$	
Fe-biochar	Monochlorobenzene/100 μM; Catalyst /100 mg L^{-1}; PMS/10 mM; pH/8.0	98.5 % in 240 min /0.017 min^{-1}	·OH; $SO_4^{\cdot-}$	[8]
N doped graphite	Yellow X-RG/200 mg L^{-1}; Catalyst /0.4 g L^{-1}; PMS/0.4 g L^{-1}; pH/8.4	92.6 % in 25 h /0.273 h^{-1}	$^1O_2$	[9]
N, S co-doped biochar	Antibiotics/20 mg L^{-1}; Catalyst /3 g L^{-1}; PMS/5 mL L^{-1}	92.2 % in 30 min /0.062 min^{-1}	$SO_4^{\cdot-}$	[10]
g-C_3N_4	Tetracycline/20 mg L^{-1}; Catalyst /200 g L^{-1}; PMS/0.5 g L^{-1}; Anion/10 mM	100 % in 30 min /0.061 min^{-1}	$^1O_2$; ·O- 2	[11]
40%-N/CoFeX	OTC = 100 mg L^{-1}; Catalyst = 25 mg L^{-1}; PMS = 1.0 mM; pH = 3.0	100% in 60 min / 0.089 min^{-1}	·OH; $SO_4^{\cdot-}$	This work

Table S4 Leached ferric and cobalt ions in catalytic reaction by 40%-N/CoFeX.

Metal ions	**1st cycle**	**2nd cycle**	**3rd cycle**	**4th cycle**	**5th cycle**
Fe (mg L^{-1})	0.024±0.003	0.019±0.001	0.014±0.001	0.011±0.003	0.005±0.002
Co (mg L^{-1})	0.018±0.001	0.013±0.002	0.011±0.003	0.006±0.002	0.004±0.002

References

[1] J. Guo, L. Wang, X. Wei, Z.A. Alothman, M.D. Albaqami, V. Malgras, Y. Yamauchi, Y. Kang, M. Wang, W. Guan, X. Xu, Direct Z-scheme $CuInS_2/Bi_2MoO_6$ heterostructure for enhanced photocatalytic degradation of tetracycline under visible light, J. Hazard. Mater. 415 (2021) 125591.

[2] Z. Yang, X. Li, Y. Huang, Y. Chen, A. Wang, Y. Wang, C. Li, Z. Hu, K. Yan, Facile synthesis of cobalt-iron layered double hydroxides nanosheets for direct activation of peroxymonosulfate (PMS) during degradation of fluoroquinolones antibiotics, J. Clean. Prod. 310 (2021) 127584.

[3] K. Faungnawakij, N. Viriya-empikul, Catalytic behavior toward oxidative steam reforming of dimethyl ether over $CuFe_2O_4$-Al_2O_3 composite catalysts, Appl Catal A: Gen. 382 (2010) 21-27.

[4] Q. Wu, H. Yang, L. Kang, Z. Gao, F. Ren, Fe-based metal-organic frameworks as Fenton-like catalysts for highly efficient degradation of tetracycline hydrochloride over a wide pH range: Acceleration of Fe(II)/ Fe(III) cycle under visible light irradiation, Appl. Catal. B Environ. 263 (2020) 118282.

[5] Q. Wan, Z. Chen, R. Cao, J. Wang, T. Huang, G. Wen, J. Ma, Oxidation of organic compounds by PMS/CuO system: The significant discrepancy in borate and phosphate buffer, J. Clean. Prod. 339 (2022) 130773.

[6] S. Shao, X. Li, Z. Gong, B. Fan, J. Hu, J. Peng, K. Lu, S. Gao, A new insight into the mechanism in Fe_3O_4@CuO/PMS system with low oxidant dosage, Chem. Eng. J. 438 (2022) 135474.

[7] J. Xie, X. Luo, L. Chen, X. Gong, L. Zhang, J. Tian, ZIF-8 derived boron, nitrogen co-doped porous carbon as metal-free peroxymonosulfate activator for tetracycline hydrochloride degradation: Performance, mechanism and biotoxicity, Chem. Eng. J. 440 (2022) 135760.

[8] L. Yang, J. Shen, W. Zhang, W. Wu, Z. Wei, M. Chen, J. Yan, L. Qian, L. Han, J. Li, M. Gu, Hydrothermally assisted synthesis of nano zero-valent iron encapsulated in biomass-derived carbon

for peroxymonosulfate activation: The performance and mechanisms for efficient degradation of monochlorobenzene, Sci. Total Environ. 829 (2022) 154645.

[9] F. Nie, W. Xu, D. Zhang, B. Jiang, Q. Sun, J. Wang, N-doped 2D graphite-2H nanoplatelets (GNPs) with enhanced PMS activation performance: Structure-dependent performance and Catalytic Mechanism, J. Taiwan Inst. Chem. Eng. 131 (2022) 104158.

[10] Y. Zhang, M. Xu, R. He, J. Zhao, W. Kang, J. Lv, Effect of pyrolysis temperature on the activated permonosulfate degradation of antibiotics in nitrogen and sulfur-doping biochar: Key role of environmentally persistent free radicals, Chemosphere 294 (2022) 133737.

[11] H. Shi, Y. He, Y. Li, T. He, P. Luo, Efficient degradation of tetracycline in real water systems by metal-free g-C_3N_4 microsphere through visible-light catalysis and PMS activation synergy, Separ. Purif. Technol. 280 (2022) 119864.